Journal of Power Sources, 41 (1993) 263–276

Positive electrode for galvanic cells prepared by anodization of CrO_3–graphite intercalation compounds in aqueous sulfuric acid

J. M. Skowroński* and K. Jurewicz

Institute of Chemistry and Applied Electrochemistry, Technical University of Poznań, ul. Piotrowo 3, 60-965 Poznań (Poland)

(Received January 2, 1992; in revised form August 31, 1992)

Abstract

Cathode materials have been prepared in 12 M H_2SO_4 by electrochemical oxidation of CrO_3–graphite intercalation compounds (CrO_3–GICs). Striking effects appearing on cyclic potentiodynamic curves of CrO_3–GICs because of intercalation of sulfuric acid are discussed in relation to the formation of the CrO_3–graphite oxide system. Charge/discharge characteristics of these cathodes are compared with those of graphite oxide prepared from pure graphite.

Introduction

Graphite intercalation compounds (GICs) have been in the past considered as cathode materials for galvanic cells with aqueous electrolyte [1–11]. On the other hand, graphite oxide can be prepared when the resulting GIC reacts with water [12–14]. In preparing graphite oxide both the chemical [15, 16] and electrochemical [12, 17–22] methods have been used. The chemical method involves the oxidation of graphite in aqueous solutions of strong oxidants, whereas in the electrochemical method graphite is oxidized anodically. In the latter method, which in the past was less frequently employed, the process control is easier and hence chemical composition of the product is more reproducible. Graphite intercalation compounds with sulfuric acid (H_2SO_4–GICs) can also play the role of the precursors for graphite oxide [19–21, 23]. In aqueous sulfuric acid the formation of graphite oxide begins before the stage 1 H_2SO_4–GIC is reached. In 10–12 M H_2SO_4, the stage 2 H_2SO_4–GIC has been observed to transform to graphite oxide [22–24]. In general, the limiting stage number of GIC, beyond which the formation of graphite oxide occurs, increases on diluting the acid but the formation of graphite oxide can also change depending on the experimental conditions of electrochemical process [18, 21, 22]. The change of the character of bonds from ionic to covalent on passing from GIC to graphite oxide can be precisely detected by electrochemical techniques [19, 20, 22, 23]. Many encouraging results have been reported more recently on the practical application of graphite oxide as active cathode material of galvanic cells [25–27] and/or as the precursor for manufacturing the fluorinated graphite cathodes [28, 29].

*Author to whom correspondence should be addressed.

0378-7753/93/$6.00

The aim of this work is to examine the process of electrochemical oxidation of pure graphite and CrO_3–GICs in 12 M H_2SO_4 and to compare the discharge performance of the resulting materials.

Experimental

CrO_3–GICs were prepared by the solvent and the impregnation-dry method. Intercalation by the former method was carried out according to the procedure of Platzer and de la Martinière [30], using a mixture of 1 g graphite and 5 g CrO_3 in 50 cm^3 glacial acetic acid. After refluxing for 5 min the product was washed with acetone and dried to constant weight. The procedure of the impregnation-dry method has been described elsewhere in detail [31, 32]. To remove unreacted CrO_3 and lower nonintercalated chromium oxides, the product of this method was washed with boiling water and 6 M HCl at 100 °C for 1 h. Finally, washing with boiling water was continued until the Cr^{6+} ion concentration in the filtrate was lower than 5×10^{-2} μm cm^3; then the sample was washed with acetone and dried to constant weight. The preparation and the chemical analysis data of the compounds are listed in Table 1.

Unless stated otherwise, the electrochemical studies were performed in 12 M H_2SO_4 using an H-type cell in which the working and the counter electrode compartments were separated by a glass frit. The working electrode on the form of a particle bed was placed on a platinum screen. To ensure a good electrical contact between the

TABLE 1

Preparation, chemical analysis and X-ray data of CrO_3–graphite intercalation compounds

Sample[a]	Intercalation method	C/Cr	Main graphite and intercalation lines	
			d (Å)	I/I_0
A1-W1	Compound produced by impregnation-dry method [31, 32] using graphite (99.7 wt.%), from Graphitwerke Kropfmühl AG, with 95 wt.% flakes in the range 170–544 μm (sample A1)	28.1	3.35 3.52[b]	100 17
A2-AC	Compound produced by solvent method [30] using graphite flakes (99.7 wt.%), from Graphitwerke Kropfmühl AG, 170–283 μm diameter (sample A2)	43.8	3.35 3.60[c]	100 95

[a]All symbols of samples are the same as in our previous papers.

[b]This broad peak appearing in the range 3.51–3.62 Å is probably composed of many components of mixed-stage structure. Evidence for intercalation by indirect methods is summarized in ref. 33.

[c]Complete X-ray diffraction pattern is published in ref. 33.

sample particles, a short glass cylinder, closed at its bottom by a polypropylene fibre, was placed at the top of the electrode. The counter electrode was a platinum spiral whereas the reference electrode was a $Hg/Hg_2SO_4/1$ M H_2SO_4 and connected to the solution under investigation by a Luggin capillary. Cyclic potentiodynamic measurements with a scan rate 0.022 or 0.1 mV/s were initiated at the rest potential of the electrode and a potential was changed in the positive direction until the reverse potential of 0.95 or 1.15 V was reached, respectively. Then the direction of polarization was reversed and the potential was diminished down to −0.05 V. From this potential a new cycle in the positive direction was carried out. Galvanostatic measurements were carried out at the charge density of 20 mA/g and the discharge density of 4 and 2 mA/g electrode, respectively (Table 2). The discharge process was started instantly after the electrode was charged. The potential of sample versus the reference electrode was recorded continuously. The discharge process was finished when the potential −0.1 V was reached. Unless stated otherwise, all measurements were performed using the electrode weight of 50 mg. The temperature was 20 °C.

Results and discussion

CrO_3–GICs examined in this paper were prepared using the graphite of different flake dimensions (Table 1) but, similarly to the results obtained earlier in 18 M H_2SO_4 [33], this parameter appeared to have no influence on the shape of the potentiodynamic curves. The typical curves of the pristine graphite (sample A1) are shown in Fig. 1. The first cycle is to some extent different as compared with the following cycles. Based on the calculations of the charge associated with the given current peaks it may be estimated that, instead of stage 1 compound obtained in 18 M H_2SO_4 [34, 35], only stage 2 compound can be completed in 12 M H_2SO_4. After the polarization is reversed the cathodic peaks associated with the reduction of H_2SO_4–GIC are recorded and, in addition, a new peak at about 0.25 V is revealed. The latter one being the response from the anodic reactions occurring at the potential range higher than 1 V is associated with the reduction of graphite oxide. A large overpotential of the reduction of graphite oxide results from the decrease of the electrical conductivity of sample due to covalent bonds formed [20, 22, 23, 36, 37]. As can be seen in Fig. 1, this cathodic peak becomes smaller on cycling. The worsening of the charge/discharge reversibility on cycling has been suggested to arise from the distortion of graphene layers [21].

In comparison with pure graphite, several interesting differences appear on the potentiodynamic curves of CrO_3–GICs. Figure 2 represents the anodic oxidation of sample A1-W1 prepared by the impregnation-dry method. The most striking phenomenon is that during the first positive scan an abrupt cathodic jump takes place at about 0.55 V. On increasing the potential, the second smaller cathodic peak is net traced (at 0.68 V) and then the curve transfers to the anodic current side. Up to the potential of 1 V the anodic charge of all peaks is smaller, whereas over this potential, is higher as compared with the respective charges of pristine graphite. Similar cathodic jump, but only a single one, has been observed recently in 18 M H_2SO_4 for the bed CrO_3–graphite electrode [34] as well as for the CrO_3–HOPG (highly-oriented pyrolytic graphite) compound [35]. This effect has been accounted for by the opening of the graphite pockets encapsulating the intercalated chromium oxides (also small amounts of lower chromium oxides of the oxidation state of chromium lower than six are residing in CrO_3–GICs [38–40]) due to cointercalation of sulfuric acid. It has been shown earlier [34] that the cathodic jump does not appear on the potentiodynamic

TABLE 2

Charge/discharge characteristics of the electrodes

I	II	III	IV	V	VI	VII
1	Electrode symbol	A1	A2-AC		A1-W1	
2	Figure (curve)	9	9	9, 10(1)	10(2)	10(3)
3	Mass of electrode (mg)	50	50	50	100	100
4	i_{charge}(mA/$g_{electrode}$)	20	20	20	20	20
5	Q_{charge}(A s/$g_{electrode}$)	600	504	462	462	231
6	Q_{charge}(A s/$g_{graphite}$)	600	600	600	600	300
7	Oxidation state, x, of graphite (C_x^+)	13.4	13.4[a]	13.4[a]	13.4[a]	26.8[a]
8	$i_{discharge}$(mA/$g_{electrode}$)	4	4	4	2	2
9	$Q_{discharge}$(A s/$g_{electrode}$)	506	605	600	600	414
10	$\gamma_Q = Q_{discharge}/Q_{charge}$ (%)	84	120	130	130	179
11	Energy density (W h/kg)	65	95	99	100	73

[a]This value was calculated assuming that the graphite matrix was exclusively oxidized.

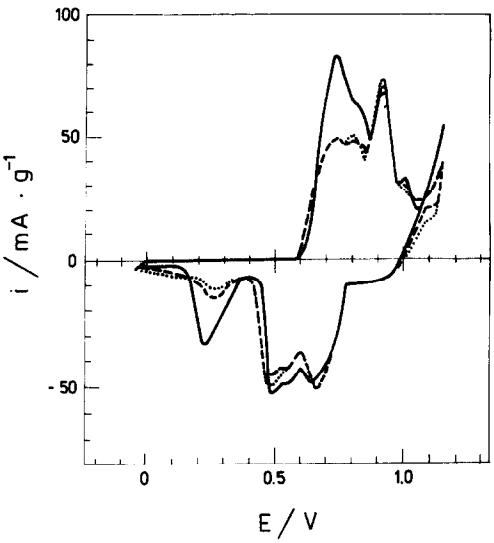

Fig. 1. Cyclic potentiodynamic curves obtained in 12 M H_2SO_4 for pristine graphite (sample A1); potential range −0.05–1.15 V, scan rate 0.1 mV/s. (——) cycle 1, (– – –) cycle 2, and (· · · · ·) cycle 3.

curves of the pristine graphite examined in sulfuric acid containing dissolved CrO_3. On this basis it may be assumed that the cathodic jumps are not associated with the chemical dissolving of CrO_3 from the compound but depend exclusively on the potential imposed on the electrode. After the reversal of polarization a large and double cathodic peak is recorded. The charge of this peak is distinctly greater as compared with the respective peak observed for the pristine graphite. The increased charge is noted until the third cycle is completed. The charge associated with this peak results from the cathodic reduction of the released CrO_3 [34].

Another interesting property of the first cathodic scan of CrO_3–GICs (Figs. 2 and 3) is that the cathodic peak associated with the reduction of graphite oxide is greater and shifted into more negative potentials (around 0.1 V) as compared with that of the pristine graphite. However, it is worth noting that on cycling this peak shifts to positive potentials whereas its charge remains almost unchanged. Figure 3 represents the results obtained for CrO_3–GIC prepared by the solvent method (sample A2-AC). As can be seen, the first anodic curve differs from that of sample A1-W1 (Fig. 2); the cathodic effects are not visible. On the other hand, there are some similarities resulting from the presence of the intercalate in the graphite structure. First, in comparison with the pristine graphite, for both compounds the increased charge is noted in the potential range corresponding to the formation of graphite oxide (over 1 V). The calculated charge is higher for sample A2-AC (Fig. 3) as compared with sample A1-W1 (Fig. 2) which is reflected in the increased cathodic charge of the current peak, with maximum at 0 V, corresponding to the reduction of graphite oxide. Secondly, during the first cycle, after the reversal of polarization, a large cathodic peak is also recorded for sample A2-AC although no cathodic jumps are recorded on the preceding anodic branch. This fact suggests that in the case of both intercalation compounds the intercalate is activated by the intercalating H_2SO_4 but there are some differences in kinetics arising from the method of intercalation.

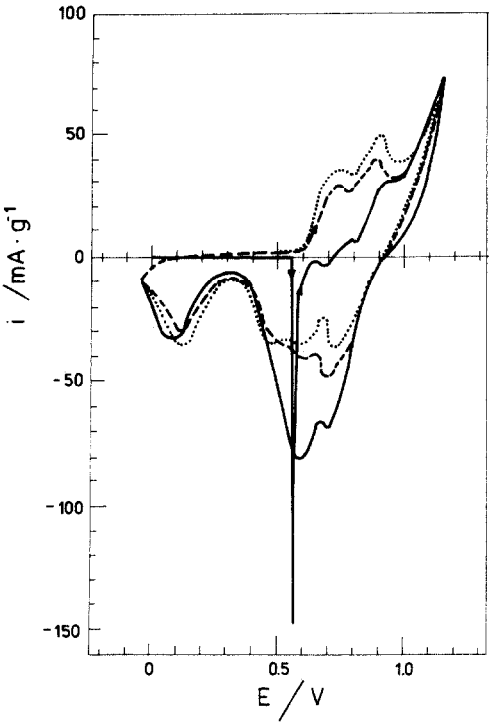

Fig. 2. Cyclic potentiodynamic curves obtained in 12 M H_2SO_4 for CrO_3–GIC (sample A1-W1); potential range −0.05–1.15 V, scan rate 0.1 mV/s. (——) cycle 1, (– – –) cycle 2, and (· · · · ·) cycle 3.

To explain more thoroughly the mentioned behaviour of CrO_3–GICs the potentiodynamic measurements were performed using a slower scan rate of 0.022 mV/s. In these conditions a very sharp cathodic jump is also recorded at about 0.6 V during the anodic sweep of sample A1-W1 but, in addition, followed by two smaller cathodic peaks at 660 and 800 mV, respectively (Fig. 4). The potential of the first cathodic jump corresponds to the potential of the onset on the potentiodynamic curve for the pristine graphite (intercalation of sulfuric acid starts) (Fig. 5). The shape of the cathodic jumps suggests that the first one at about 0.6 V is a very fast reaction whereas the following cathodic peaks are related to the diffusion rate controlled reactions. According to the mechanism proposed earlier [34, 35], the major jump is associated with opening the graphite pockets encapsulating the intercalate islands. The intercalate released and/or reacting with the cointercalating H_2SO_4 and then hydrolyzed results in the increase in the sample potential over that of the generator. In consequence, the cathodic reaction takes place instantly. In the case of sample A2-AC only the last cathodic jump at about 0.8 V is recorded (Fig. 6) because the rest potential of this electrode is higher than the potentials corresponding to the first two peaks noted for sample A1-W1.

The presence of CrO_3 intercalated in the graphite lattice leads to the changes in the galvanostatic curves. As can be seen in Fig. 7, the curve obtained for the pristine graphite demonstrates several steps associated with the intercalation of H_2SO_4 into

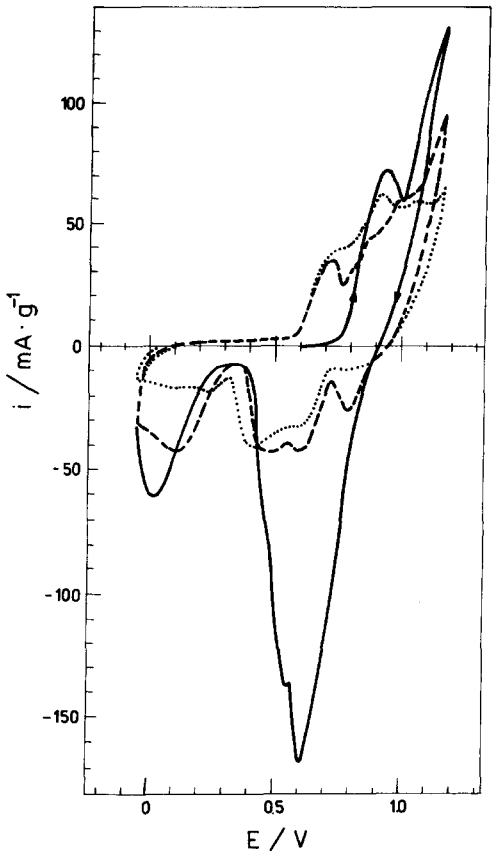

Fig. 3. Cyclic potentiodynamic curves obtained in 12 M H_2SO_4 for CrO_3–GIC (sample A2-AC); potential range −0.05–1.15 V, scan rate 0.1 mV/s. (——) cycle 1, (– – –) cycle 2, and (· · · · ·) cycle 3.

graphite followed by the set of low frequency oscillations resulting from the competition between the formation of H_2SO_4–GIC and its decomposition ('hydrolysis') to graphite oxide [22–24]. These oscillations begin to start when stage 2 H_2SO_4–GIC is completed and disappear after the anodic charge of about 2200 A s/g is passed. The first potential peak appearing at 1.05 V corresponds to the oxidation state of C_{38}^+. At this potential the onset on the potentiodynamic curves corresponding to the formation of graphite oxide is demonstrated (Fig. 1).

In the case of CrO_3–GICs (Fig. 8) the stepped part of the galvanostatic curve is distinctly shortened (anodic charge per carbon atom is about twice smaller) as compared with that in Fig. 1. Similar effect of the intercalated CrO_3 has been noted in 18 M H_2SO_4 [34] and was attributed to the chemical assistance of the process by the released CrO_3. After reaching the potential of 0.97 V the curves of CrO_3–GICs, prepared by the impregnation-dry as well as the solvent method, transfer to the plateaus and no oscillations are noted. Taking into account the fact that the potential drop coincides with the decrease in the electrical conductivity of the sample due to the formation of covalent bonds of graphite oxide followed by the hindered diffusion of water into

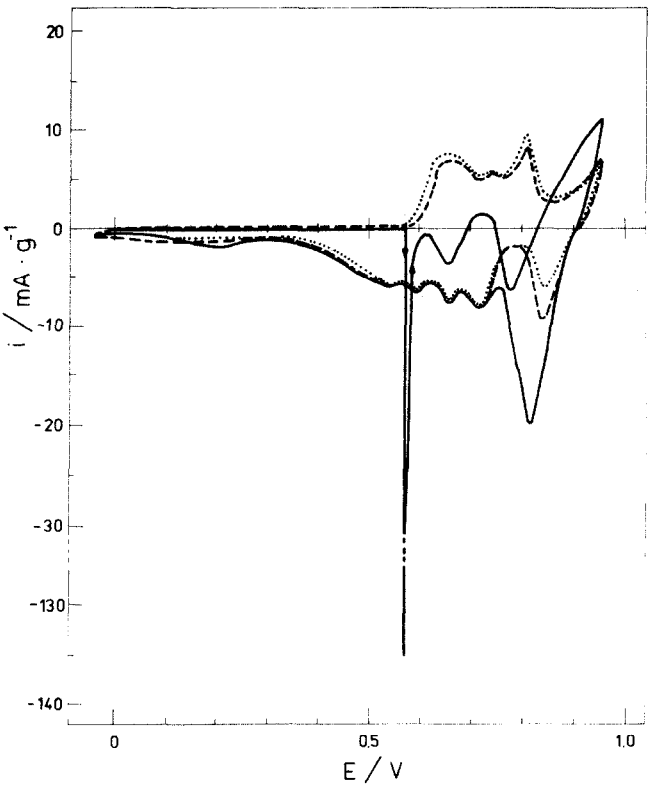

Fig. 4. Cyclic potentiodynamic curves obtained in 12 M H_2SO_4 for CrO_3–GIC (sample A1-W1); potential range −0.05–0.95 V, scan rate 0.022 mV/s. (——) cycle 1, (– – –) cycle 2, and (· · · · ·) cycle 3.

the graphite lattice [23, 24], it can be drawn that the reaction mechanism changes when CrO_3–GIC is used instead of pure graphite. It seems plausible that the intercalated as well as the released CrO_3 influences on the oxidative and the transport properties of the system. It was observed that during the overoxidation of CrO_3–GICs the peripheral regions of graphite flakes exfoliated and the bed electrode swelled. On this basis, it may be assumed that the worsening of the structural perfection of the graphene layers and the increase in ohmic polarization of the electrode are, among others, responsible for the disappearance of oscillations on the galvanostatic curves. As can be seen in Fig. 8, contrary to the compound prepared by the solvent method (sample A2-AC), the compound obtained by the impregnation-dry one (A1-W1) exhibits two plateaus. The under one is tentatively assumed to arise from the oxidation reaction of lower chromium oxides intercalated in this sample [38–40]. The problem still remains to be considered in the future whether during the formation of graphite oxide the intercalated chromium oxides are completely deintercalated or can be retained in the graphite oxide structure.

Figures 9 and 10 compare the charge/discharge characteristics of the pristine graphite and CrO_3–GICs. The charge curves presented in Fig. 9 were obtained in such a way that all samples were oxidized with the same anodic charge in relation

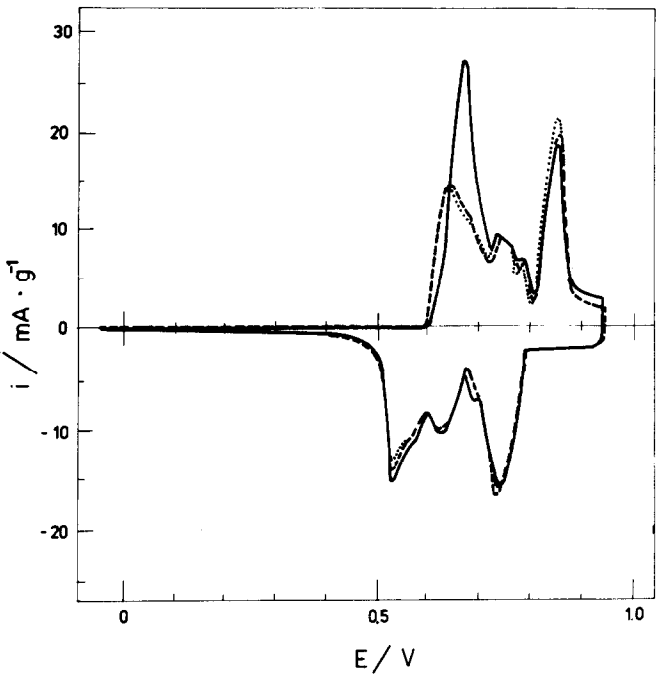

Fig. 5. Cyclic potentiodynamic curves obtained in 12 M H_2SO_4 for pristine graphite (sample A1); potential range −0.05–0.95 V, scan rate 0.022 mV/s. (——) cycle 1, (– – –) cycle 2, and (· · · · ·) cycle 3.

to the weight of carbon contained in the electrode whereas the discharge process was started immediately after the charge of the electrode was finished. The oscillations present on the charge curve of the pristine graphite make it clear that H_2SO_4–GIC coexists with graphite oxide even at the end of this partial charging. Figure 9 shows, on the other hand, that the discharge capacity of both electrodes based on CrO_3–GICs (A2-AC and A1-W1) exceeds that of the electrode of the pristine graphite (A1). The capacity efficiency defined as γ_Q = discharge capacity/charge capacity, is also distinctly higher for the electrodes of the graphite intercalated with CrO_3 (Table 2). The discharge curve of electrode A1 is composed of several steps corresponding to the deintercalation of H_2SO_4–GIC and of a large plateau at about 0.4 V associated with the reduction of the graphite oxide. For electrodes A2-AC and A1-W1 the mentioned stepped section is preceded by the first plateau at the potential of about 0.9 V probably related to the reduction of hexavalent chromium. The second shorter plateau (about 0.2 V) with the tendency to incline appears at the potential lower than that of sample A1. This difference is probably effected by the increased electrical resistance of the expanded bed of these electrodes. It is believed that this part of characteristic will undergo a change for the better using the compacted or the plastic bonded electrodes. In spite of the present disadvantage the energy density of the cathodes originated from CrO_3–GICs appeared considerably higher as compared with that of the graphite based cathode. The results of the calculations presented in Table 2 (columns III–VI) show that the mentioned profit is about 50%. It is likely that the use of a new type of electrodes

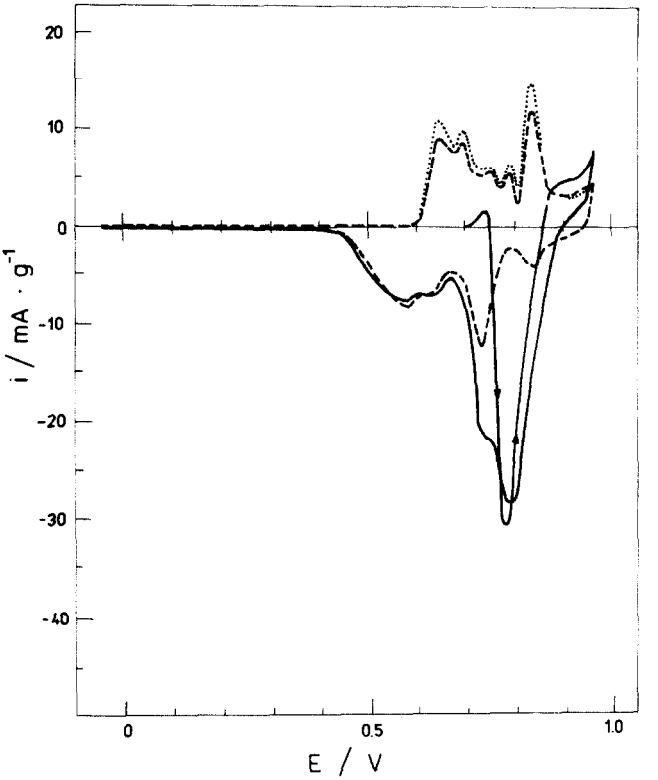

Fig. 6. Cyclic potentiodynamic curves obtained in 12 M H_2SO_4 for CrO_3–GIC (sample A2-AC); potential range 0.05–0.95 V, scan rate 0.022 mV/s. (——) cycle 1, (– – –) cycle 2, and (· · · · ·) cycle 3.

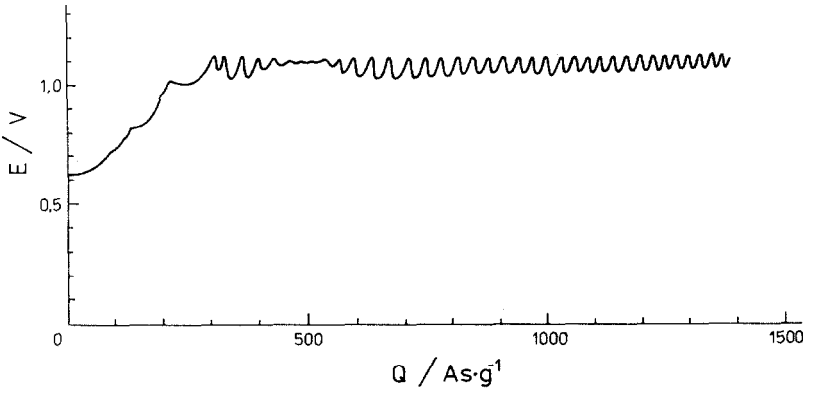

Fig. 7. Galvanostatic oxidation of pristine graphite (sample A1) in 12 M H_2SO_4 with current density 4 mA/g, $m = 50$ mg.

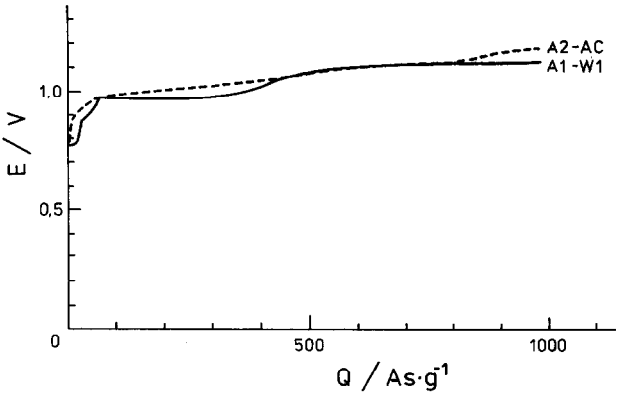

Fig. 8. Galvanostatic oxidation of CrO_3–GICs (samples A1-W1 and A2-AC) in 12 M H_2SO_4 with current density 4 mA/g, $m = 50$ mg.

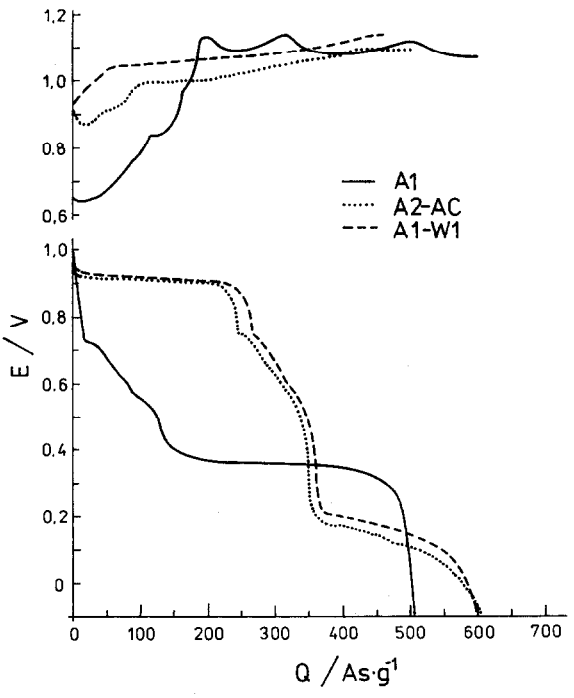

Fig. 9. Charge/discharge curves of pristine graphite (sample A1) and CrO_3–GICs (samples A1-W1 and A2-AC) in 12 M H_2SO_4; $m = 50$ mg, $i_{charge} = 20$ mA/g, and $i_{discharge} = 4$ mA/g.

will make it possible to estimate both the maximum charge of the examined cathodes and the cathode reversibility on cycling.

At this point it is reasonable to answer a question of why the discharge capacities of the cathodes prepared from CrO_3–GICs of significantly different chromium content (this ratio for samples A1-W1 and A2-AC equals 1.4) are almost the same. To approach

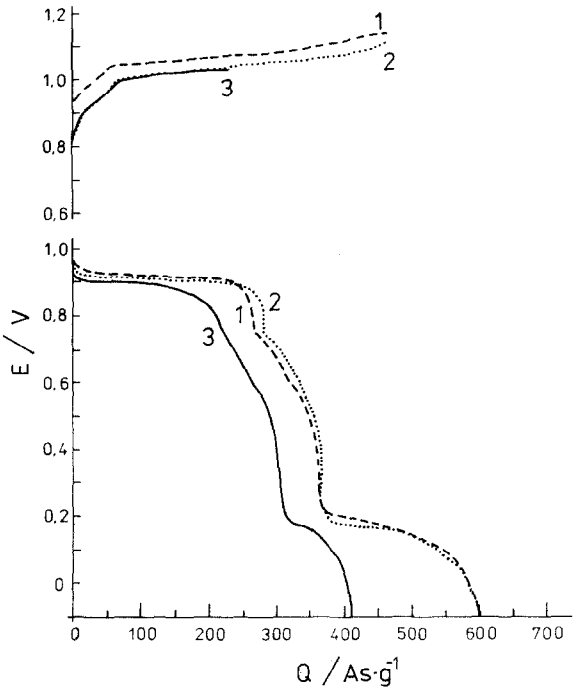

Fig. 10. Charge/discharge curves of CrO_3–GIC (sample A1-W1) in 12 M H_2SO_4. i_{charge} of all electrodes = 20 mA/g. (1) $i_{discharge}$ = 4 mA/g, m = 50 mg, (2) $i_{discharge}$ = 2 mA/g, m = 100 mg, and (3) $i_{discharge}$ = 2 mA/g, m = 100 mg.

this problem, the results of the previous works [32, 33, 38–41] on the influence of the method of intercalation on the composition and the structural properties of both compounds should be taken into account. Briefly speaking, the compounds of the impregnation-dry method are more disordered and the intercalate is more resistant to deintercalation as compared with the solvent method compounds. Assuming that within the plateau positioned at 0.9 V the reduction of the intercalate occurs from $Cr^{6+} \rightarrow Cr^{3+}$, then the calculated amounts of the reduced intercalate, in relation to the total amount of the intercalate before the discharge is started, are equal to 39.1 wt.% for sample A1-W1 and 49.8 wt.% for sample A2-AC, respectively. This result suggests that the rest of the intercalate still remains in the graphite pockets as nonreduced molecules and/or is dissolved in the electrolyte. On the basis of the cyclic potentiodynamic curves of CrO_3–GICs it may be inferred that the former case is more prevailing. Figures 2–4 and 6 show that the cathodic peak starting at about 0.9 V, after the polarization is reversed to the negative direction, and associated with the reduction of Cr^{6+}, does not disappear during the first cycle. The result also consistent with the above interpretation is that during the first cycle more intercalate is reduced from sample A2-AC whereas sample A1-W1 renders his intercalate accessible to the cathodic reduction gradually during several cycles. This problem is now under investigation to provide more quantitative results related to the reversibility of the system.

Figure 10 referring to the CrO_3–GIC electrode (A1-W1) shows how the discharge characteristics change depending on the degree of electrode charging (the oxidation state of graphite). The most interesting observation is that very beneficial to an

improvement of the capacity efficiency, γ_Q, appears the decreased charging of electrode (Table 2, columns VI and VII). The comparison of curves 2 and 3 in Fig. 10 allows to state that, for less charged cathode, the charge exhausted due to the reduction of CrO_3 exceeds the reduction of charge arising form the discharge of graphite oxide. This result is encouraging to study a wide range of experimental conditions in order to achieve the most efficient utilization of the CrO_3–graphite oxide cathodes.

The results of this work show that the electrochemical preparation of graphite oxide by using CrO_3–GICs differs from that using pure graphite. In order to understand comprehensively the reaction mechanism the further studies, particularly related to the changes taking place in the structure and composition of CrO_3–GICs during the charge/discharge cycling as well as to the role of chromium ions leached out from the GIC lattice, are now developed.

Acknowledgements

Financial support of this work by the Polish Ministry of Education (Grant No. DNS-T/09/147/90-2 is gratefully acknowledged.

References

1 S. Flandrois, J. M. Masson and J. C. Rouillon, *Synth. Methods, 3* (1981) 195.
2 F. Beck, H. Junge and H. Krohn, *Electrochim. Acta, 26* (1981) 799.
3 S. Flandrois, *Synth. Methods, 4* (1982) 255.
4 F. Beck, H. Krohn and W. Keiser, *J. Appl. Electrochem., 12* (1982) 505.
5 F. Beck, H. Krohn and W. Keiser, *J. Electroanal. Chem., 165* (1984) 93.
6 Ph. Touzain, *Ann. Phys., 11* (1986) 23.
7 J. M. Skowroński, in L. J. Pearce (ed.), *Power Sources 11,* Int. Power Sources Symp. Committee, Leatherhead, UK, 1987, p. 329.
8 J. M. Skowroński, *J. Power Sources, 25* (1989) 133.
9 J. M. Skowroński, *J. Appl. Electrochem., 19* (1989) 287.
10 J. M. Skowroński, *Mater. Chem. Phys., 24* (1990) 269.
11 N. Iwashita and M. Inagaki, *Electrochim. Acta, 36* (1991) 591.
12 W. Rüdorff and U. Hofmann, *Z. Anorg. Allg. Chem., 238* (1938) 1.
13 M. J. Bottomley, G. S. Parry, A. R. Ubbelohde and D. A. Young, *J. Chem. Soc.,* (1963) 5674.
14 H. P. Boehm, M. Eckel and W. Scholtz, *Z. Anorg. Allg. Chem., 353* (1967) 236.
15 B. C. Brodie, *Ann. Chim. Phys., 45* (1855) 251.
16 H. P. Boehm and W. Scholtz, *Liebigs Ann. Chem., 691* (1966) 1.
17 B. K. Brown and O. W. Storey, *Trans. Am. Chem. Soc., 53* (1928) 129, 140.
18 J. O. Besenhard and H. P. Fritz, *Z. Anorg. Allg. Chem., 416* (1975) 106.
19 H. Krohn, F. Beck and W. Herrman, *Chem.-Ing.-Techn., 54* (19820 510.
20 J. O. Besenhard, E. Wudy, H. Möhwald, J. J. Nickl, W. Biberacher and W. Foag, *Synth. Methods, 7* (1983) 185.
21 J. O. Besenhard, P. Minderer and M. Bindl, *Synth. Methods, 34* (1989) 133.
22 F. Beck and H. Krohn, in S. Shavangapani, J. R. Akridge and B. Schlimm (eds.), *The Electrochemistry of Carbon,* The Electrochemical Society, Pennington, NJ, 1984, pp. 574–594.
23 J. O. Besenhard, M. Bindl and H. Möhlwald, in *Proc. 4th Int. Carbon Conf., Baden-Baden, 1986,* p. 414.
24 A. Harrach, J. Douglade and A. Metrot, *Mater. Science Forum, 91–93* (1992) 689–693.
25 Ph. Touzain and R. Yazami, *J. Power Sources, 14* (1985) 89.

26 R. Yazami and Ph. Touzain, *Synth. Methods, 12* (1985) 499.
27 M. Mermoux, R. Yazami and Ph. Touzain, *J. Power Sources, 20* (1987) 105.
28 T. Nakajima, R. Hagiwara, K. Moriya and N. Watanabe, *J. Electrochem. Soc., 133* (1986) 1761.
29 T. Nakajima, A. Mabuchi, R. Hagiwara and N. Watanabe, *J. Electrochem. Soc., 135* (1988) 273.
30 N. Platzer and B. de la Martinière, *Bull. Soc. Chim. Fr., 197* (1961) 177.
31 J. M. Skowroński, *Electrochim. Acta, 30* (1985) 989.
32 J. M. Skowroński, *Carbon, 24* (1986) 185.
33 J. M. Skowroński, *Carbon, 27* (1989) 537.
34 J. M. Skowroński and K. Jurewicz, *Synth. Methods, 40* (1991) 161.
35 J. M. Skowroński, J. Douglade and A. Metrot, *Mater. Science Forum, 91–93* (1992) 659–664.
36 J. E. Fischer, A. Metrot, P. J. Flanders, W. R. Salanek and C. F. Brucker, *Phys. Rev. B, 23* (1981) 10-5576.
37 A. Harrach, C. Nicollin and A. Metrot, *Synth. Methods, 34* (1989) 467.
38 J. M. Skowroński, *Electrochim. Acta, 32* (1987) 1285.
39 J. M. Skowroński, *Synth. Methods, 22* (1987) 157.
40 J. M. Skowroński, *Electrochim. Acta, 33* (1988) 953.
41 J. M. Skowroński, *Carbon, 26* (1988) 613.